Journal of Advanced Research 34 (2021) 173–186

Contents lists available at ScienceDirect

Journal of Advanced Research

journal homepage: www.elsevier.com/locate/jare

Calenduloside E suppresses calcium overload by promoting the interaction between L-type calcium channels and Bcl2-associated athanogene 3 to alleviate myocardial ischemia/reperfusion injury

Ruiying Wang [a,b,c], Min Wang [a,b,c], Jiahui Zhou [a,b,c], Ziru Dai [a,b,c], Guibo Sun [a,b,c,*], Xiaobo Sun [a,b,c,*]

[a] Institute of Medicinal Plant Development, Chinese Academy of Medical Sciences & Peking Union Medical College, Beijing 100193, China
[b] Beijing Key Laboratory of Innovative Drug Discovery of Traditional Chinese Medicine (Natural Medicine) and Translational Medicine, Institute of Medicinal Plant Development, Peking Union Medical College & Chinese Academy of Medical Sciences, Beijing 100193, China
[c] Key Laboratory of New Drug Discovery Based on Classic Chinese Medicine Prescription, Chinese Academy of Medical Sciences, Beijing 100193, China

GRAPHICAL ABSTRACT

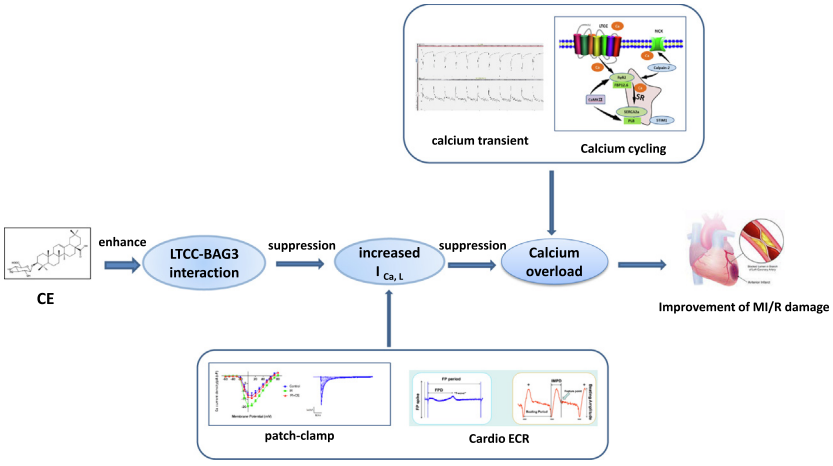

ARTICLE INFO

Article history:
Received 6 July 2020
Revised 22 October 2020
Accepted 26 October 2020
Available online 31 October 2020

Keywords:
Calenduloside E
Myocardial ischemia/reperfusion injury
L-type calcium channels
Calcium overload
Bcl2-associated athanogene 3

ABSTRACT

Introduction: Intracellular calcium overload is an important contributor to myocardial ischemia/reperfusion (MI/R) injury. Total saponins of the traditional Chinese medicinal plant *Aralia elata* (Miq.) Seem. (AS) are beneficial for treating MI/R injury, and Calenduloside E (CE) is the main active ingredient of AS.
Objectives: This study aimed to investigate the effects of CE on MI/R injury and determine its specific regulatory mechanisms.
Methods: To verify whether CE mediated cardiac protection in vivo and in vitro, we performed MI/R surgery in SD rats and subjected neonatal rat ventricular myocytes (NRVMs) to hypoxia-reoxygenation (HR). CE's cardioprotective against MI/R injury was detected by Evans blue/TTC staining, echocardiography, HE staining, myocardial enzyme levels. Impedance and field potential recording, and patch-clamp techniques of human-induced pluripotent stem cell-derived cardiomyocytes (hiPSC-CMs) were used to detect the function of L-type calcium channels (LTCC). The mechanisms underlying between CE and LTCC was

Peer review under responsibility of Cairo University.
* Corresponding authors at: Institute of Medicinal Plant Development, Chinese Academy of Medical Sciences & Peking Union Medical College, No. 151 Malianwa North Road, Haidian District, Beijing, China.
E-mail addresses: sunguibo@126.com (G. Sun), sun_xiaobo163@163.com (X. Sun).

https://doi.org/10.1016/j.jare.2020.10.005

studied through western blot, immunofluorescence, and immunohistochemistry. Drug affinity responsive target stability (DARTS) and co-immunoprecipitation (co-IP) used to further clarify the effect of CE on LTCC and BAG3.

Results: We found that CE protected against MI/R injury by inhibiting calcium overload. Furthermore, CE improved contraction and field potential signals of hiPSC-CMs and restored sarcomere contraction and calcium transient of adult rat ventricular myocytes (ARVMs). Moreover, patch-clamp data showed that CE suppressed increased L-type calcium current ($I_{Ca,L}$) caused by LTCC agonist, proving that CE could regulate calcium homeostasis through LTCC. Importantly, we found that CE promoted the interaction between LTCC and Bcl2-associated athanogene 3 (BAG3) by co-IP and DARTS.

Conclusion: Our results demonstrate that CE enhanced LTCC-BAG3 interaction to reduce MI/R induced-calcium overload, exerting a cardioprotective effect.

Introduction

Ischemic heart disease is characterised by high morbidity and mortality. Following ischemia, reperfusion via thrombolysis, induced by surgery or medication, may further promote cardiac damage, a phenomenon which is known as myocardial ischemia/reperfusion (MI/R) injury [1]. The mechanisms underlying MI/R injury have not yet been fully elucidated. Different factors, including energy metabolism disorders, oxidative stress, calcium overload, myocardial cell apoptosis, and vascular endothelial cell dysfunction are considered crucial in MI/R injury [2]. Calcium overload occurs during reperfusion and damages cardiomyocytes through various mechanisms [1]. In fact, calcium overload directly induces cardiac systolic dysfunction, and can promote cellular apoptosis and myocardial injury, which is the most unfavourable consequence for patients with ischemic heart disease [3]. Therefore, identifying reagents that could ameliorate MI/R injury by reducing calcium overload is essential.

L-type calcium channels (LTCC) are located on several electrically excitable tissues, especially the heart, and include the four isoforms $Ca_v1.1$, $Ca_v1.2$, $Ca_v1.3$, and $Ca_v1.4$ [4]. In myocardial cells, LTCC opening causes entry of extracellular calcium into the cell, which triggers the release of a considerable amount of calcium through ryanodine receptor 2 (RyR2) from the sarcoplasmic reticulum (SR), thereby inducing contraction of cardiac myocytes [5]. LTCC communicates with RyR2 and participates in excitation–contraction coupling [6]. Besides, calcium channel blockers, such as nifedipine, nisoldipine, and diltiazem, are used clinically in the treatment of hypertension and coronary heart disease. LTCC is known to initiate calcium cycling and calcium overload is considered the main damage induced by MI/R, so the specific mechanisms by which LTCC regulates MI/R was further explored in this study.

Aralia elata (Miq.) Seem. is a well-known traditional Chinese medicinal plant used for treatment of arrhythmia, diabetes, and coronary heart disease [7]. Previously, we proved that total saponins of *Aralia elata* (Miq.) Seem. (AS) exhibit anti-myocardial ischemia, anti-hypoxia, and anti-endothelial injury activity [8,9]. Calenduloside E (CE), a natural pentacyclic triterpenoid saponin, is the main active ingredient of AS. Our team demonstrated that CE protects H9c2 cardiomyocytes against oxidative damage and reduces apoptotic injury of human umbilical vein endothelial cells (HUVECs) [10]. Moreover, CE can alleviate the damage caused by arrhythmia in a variety of models, and regulates calcium and sodium channels to illustrate the mechanism of treating arrhythmias. Notably, our previous study concluded that AS could play cardiac protective role by inhibiting calcium overload and improve contraction function of myocardial cells [8]. Studies have shown that dihydropyridine calcium antagonists, such as furnidipine and diltiazem, can reduce myocardial ischemia–reperfusion injury by inhibiting apoptosis and oxidative stress [11,12]. Our research has proved that CE can play a cardioprotective effect by reducing calcium overload. CE plays a role similar to calcium antagonists, but its specific mechanisms are not exactly the same as calcium antagonists. So, we began to study the protective mechanism of CE against MI/R injury from the perspective of calcium overload.

In this study, we evaluated the effects of CE on MI/R injury in rats and hypoxia-reoxygenation (HR) injury in hiPSC-CMs and NRVMs. Importantly, the present study aimed to illuminate the underlying mechanisms of CE-mediated calcium overload inhibition and cardiac protection.

Materials and methods

Experimental materials

CE (Fig. 1b) were provided by the Institute of Medicinal Plant Development (Beijing, China) [9,10]. Bay-K-8644 (S7924) and nisoldipine (S1748) were purchased from Selleck (Shanghai, China). The primary antibodies in this article were used including: SERCA (ab2861, 1:1000), RyR2 (ab2868, 1:1000), NCX (ab177952, 1:1000), α1C (ab84814, 1:1000), calpain-2 (ab126600, 1:1000), STIM1 (ab57834, 1:1000), CaMKII (ab22609, 1:1000), p-CaMKII (ab32678, 1:1000), p-PLB (ab15000, 1:1000), calmodulin (ab45689, 1:1000), Troponin I (ab52862, 1:1000) and tubulin (ab6046, 1:2000) were purchased from abcam (Cambridge, UK); FKBP12.6 (sc-376135, 1:200) and PLB (sc-393990, 1:200) were purchased from Santa Cruz Biotechnology (California, USA); BAG3 (A14826, 1:500), α2δ (A10315, 1:500), γ (A10014, 1:500) and β (A9304, 1:500) were purchased from ABclonal (Wuhan, China). The secondary antibodies in this article were used including: rabbit (ab6721, 1:2000) and mouse (ab6728, 1:2000).

Animals and MI/R injury model

Animal studies conformed to the ARRIVE guidelines [13]. Adult Sprague Dawley (SD) rats were housed for three days before experiments under standard laboratory conditions. All experimental operations were approved by the Laboratory Animal Ethics Committee of the Institute of Medicinal Plant Development, Peking Union Medical College (No. SLXD-20190614006), and conformed to the Guide for the Care and Use of Laboratory Animals. All SD rats were purchased from Beijing Vital River Laboratory Animal Technology Co., Ltd (Beijing, China).

SD male rats (270–280 g) were anaesthetised by intraperitoneal injection of sodium pentobarbital (50 mg/kg). Following tracheal intubation, the rats breathed with a ventilator, and were then fixed in supine position and connected to the electrocardiogram. The chest was then opened, and the left anterior descending (LAD) coronary artery was ligated over a tube with a thread from 2 mm below the left atrial appendage [14]. Heart ischemia began when

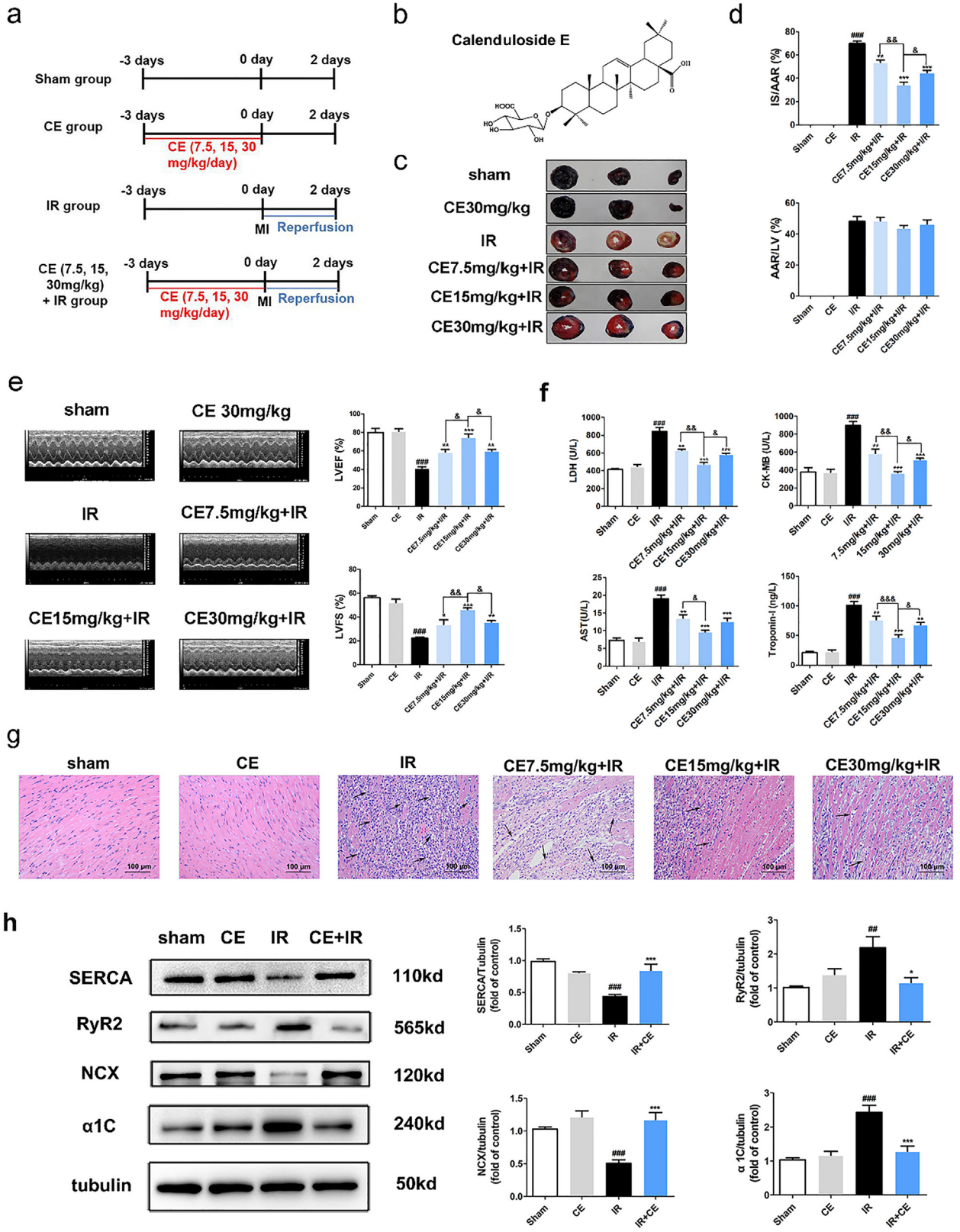

Fig. 1. CE attenuated myocardial ischemia/reperfusion (MI/R) injury in rats by suppressing calcium overload. After CE (7.5, 15, 30 mg/kg) treatment for three days, the rats have undergone IR surgery. (a) Experimental protocol 1 to detect the effects of CE on MI/R injury in rat. (b) The molecular structure of Calenduloside E (CE). (c) The myocardial infarction area was detected by Evans Blue/TTC staining. (d) The quantification of infarct size (IS/AAR) and ischemic size (AAR/LV) was also displayed (n = 5 per group). (e) Representative trace of M−mode echocardiography performed 48 h after MI/R injury in a rat study and quantitative analysis of left ventricular ejection fraction (LVEF) and left ventricular fractional shortening (LVFS) using echocardiography (n = 5 per group). (f) The levels of LDH, AST, CK-MB, and Troponin-I were detected (n = 5 per group). (g) The myocardial pathological damage was detected by HE staining (scale bar, 100 μm, n = 5 per group) and black arrows indicated inflammatory cell infiltration. (h) The representative western blot bands and quantitation of SERCA, RyR2, NCX, and α1C in rat myocardial tissue (n = 5 per group). The data were expressed as the mean ± SD. $^{###}P < 0.001$ vs sham group; $^{*}P < 0.05$ vs IR group, $^{**}P < 0.01$ vs IR group, $^{***}P < 0.001$ vs IR group; $^{\&}P < 0.05$, $^{\&\&}P < 0.01$.

the ST segment of the ECG raised, and lasted for 30 min, as previously reported. In sham group and CE group, LAD coronary arteries were not ligated to the tube; all other procedures were the same as the IR group. Following ischemia, the hearts were perfused for 48 h. After the operation, the ventilator was removed when the rats were able to breathe spontaneously. They were then placed on a thermostatic blanket until they could walk, and were returned to the cage.

Experimental protocols with rats

In all experiments, rats were randomly divided into groups.

Experiment protocol 1 (Fig. 1a): Ninety rats were divided equally into six groups: sham, CE, IR, CE (7.5 mg/kg) + IR, CE (15 mg/kg) + IR, and CE (30 mg/kg) + IR. Sham and IR groups were given an equal volume of ultrapure water containing 0.5‰ sodium carboxymethylcellulose intra-gastrically for three days. Treatment groups were administered 7.5, 15, or 30 mg/kg CE intra-gastrically for three days and the last treatment finished 60 min before MI/R injury model. Then proceed the next experiments, including Evans Blue/TTC (n = 5), HE (n = 5) and western blot (n = 5).

Experiment protocol 2 (Fig. 4a): Seventy five rats were divided equally into five groups: sham, IR, IR + CE, IR + CE + Bay-K-8644, IR + nisoldipine. Sham and IR groups were given an equal volume of ultrapure water containing 0.5‰ sodium carboxymethylcellulose intra-gastrically for three days and saline by intravenous injection in the tail 30 min before surgery. Treatment groups we administered 15 mg/kg CE and 2 mg/kg nisoldipine intra-gastrically for three days and injected 30 μg/kg Bay-K-8644 in the tail vein 30 min before MI/R injury model. Then proceed the next experiments, including Evans Blue/TTC (n = 5), immunohistochemistry (n = 5) and western blot (n = 5).

Infarct size measurement

The experimental protocols are shown in Fig. 1a and Fig. 4a. Infarct size after MI/R injury was determined by Evans Blue/triphenyl tetrazolium chloride (TTC) staining, as described previously [15]. After MI/R, the rat heart was re-ligated in the original position, and then 2% Evans Blue was slowly injected from the abdominal aorta. After 1 min, rat hearts were removed, frozen, and cut into 2-mm slices along the heart axis. The tissue was then stained in 1% TTC (93140, Sigma-Aldrich Corp., St. Louis, MO USA) solution at 37 ℃ and fixed with 4% paraformaldehyde. White staining indicates myocardial infarction size (IS), bright red staining indicates area at risk (AAR), blue staining indicates non-ischemic region. The proportion of the infarcted area was counted after obtaining tissue images.

Cardiac function measurement by echocardiography

Cardiac function was assessed using M−mode echocardiography. Briefly, rats were anesthetized with 2% isoflurane, and echocardiography was performed using a Vevo 770 high-resolution in vivo imaging system (FUJIFILM VisualSonics, Inc., Toronto, Ontario, Canada). M−mode tracing of the left ventricle was obtained from the parasternal long-axis view. Left ventricular ejection fraction (LVEF) and left ventricular fractional shortening (LVFS) were calculated using computer algorithms.

Myocardial injury indicators of rat serum determination

The experimental protocols are shown in Fig. 1a and Fig. 4a. After treatment, the sera of SD rats were collected to detect the levels of Troponin I, Creatine Kinase-MB (CK-MB), lactate dehydrogenase (LDH) and aspartate aminotransferase (AST) using commercial ELISA kits (Beijing Expandbiotech Ltd., Beijing, China) according to the manufacturer's instructions. The absorbance of each well was measured at 450 nm using a Synergy H1 microplate reader (BioTek, Vermont, USA).

Histopathological detection

The experimental protocols are shown in Fig. 1a. After MI/R, rat hearts were fixed in 4% paraformaldehyde and embedded in paraffin after dehydration. The embedded tissue was cut into 5–8 μm sections, which were attached to a glass slide. The sections were heated, deparaffinised, and dehydrated before staining with haematoxylin and eosin (HE). The images were acquired by Aperio S2 Leica Biosystem microscopy (Leica, Wetzlar, Germany).

Adult rat ventricular myocyte (ARVM) isolation and Ca^{2+} transient measurement

The experimental protocols are shown in Fig. 1a. After treatment, rat hearts were removed and hung on the Langendorff perfusion system. Left ventricle of heart was then dispersed into individual cardiomyocytes by perfusing type II collagenase, followed by grinding, as previously reported [7]. Cardiomyocytes that appeared rod-shaped (more than 85%) under the microscope could be used for subsequent experiments. Next, video-based sarcomere contractility and calcium recording module in a SoftEdge MyoCam System (IonOptix Corporation, Milton, MA, USA) were used to detect sarcomere shortening and Ca^{2+} transient-related indicators, simultaneously. Cardiomyocytes were incubated with Fura-2 AM (2 μM) for 20 min in a dark environment. Then, the cardiomyocytes were placed in a cell perfusion chamber on an inverted microscope stage and stimulated by an electric field (0.5 Hz, 5 ms). Sampling speed in this experiment reached 1000 times/s. The indicators related to sarcomere shortening (including resting sarcomere length, maximal velocity of re-lengthening (-dL/dt), maximal velocity of shortening (+dL/dt), sarcomere shortening amplitude, the time-to-peak shorting (TPS) and the time-to-90% re-lengthening (TR90)) and Ca^{2+} transients (including resting calcium levels, calcium relaxation maximal velocity (-d $[Ca^{2+}]/dt_{max}$), calcium shorting maximal velocity (+d $[Ca^{2+}]/dt_{max}$), calcium amplitude, Time-to-50% peak $[Ca^{2+}]$, intracellular calcium transient decay rate) were collected and recorded by the IonWizard 6.0 software in real-time (n = 16/group).

Simultaneous detection of beat signals and potential signals of (human-induced pluripotent stem cell-derived cardiomyocytes) hiPSC-CMs

HiPSC-CMs were purchased from Cellapybio (CA2201106, Beijing, China). The e-plate was covered with 1% Matrigel at 37 ℃ overnight. The cells were thawed quickly in a 37 ℃ water bath and seeded at 3×10^4 cells/well on the e-plate after removing the Matrigel. Fresh medium was supplied the next day and then changed every two days. The e-plates can be placed on the xCELLigence RTCA Cardio ECR System to detect the beat signals and potential signals of hiPSC-CMs [16]. The drug treatment started when the beat signals and potential signals stabilised.

Control and HR groups were cultured in normal medium containing 1‰ DMSO. In the treatment group, hiPSC-CMs were cultured in medium containing 2, 4, or 8 μM CE and 0.1 μM nisoldipine before inducing hypoxia for 5 h and reoxygenation for 24 h, and 8 nM Bay-K-8644 was added 2 h before HR.

Patch-clamp detection

Calcium currents were recorded using whole-cell voltage-clamp techniques (EPC10 amplifier, HEKA, USA). For L-type calcium current ($I_{Ca,L}$) recordings, the pipette solution and the bath solution contained the following (mM): CsCl 120, $MgCl_2$ 1, HEPES 10, Mg-ATP 4, EGTA 10, Na_2-GTP 0.3 (pH 7.2 with CsOH), and the bath solution contained the following (mM): TEA-Cl 140, $MgCl_2$ 2, $CaCl_2$ 10, HEPES 10, Glucose 5, (pH 7.4 with TEA-OH. Currents were digitised at a sampling rate of 5 kHz. At 10 mV step depolarizations, $I_{Ca,L}$ was recorded from a holding potential of −60 mV, between −60 and + 60 mV. The steady-state inactivation curve was obtained by a 250-ms test pulse to 10 mV, after a pre-pulse of 2000 ms from −60 mV to + 80 mV, by 10 mV steps. Recovery from inactivation was analysed by two steps. From a holding potential of −60 mV, the membrane was first pulsed to 10 mV for 250 s to induce inactivation. The membrane was then repolarised to −90 mV for varying periods before the second pulse to 10 mV for 250 ms was applied [17]. The hiPSC-CMs and ARVMs were used for patch-clamp, the experiment protocols of cell culture were the same as above.

Neonatal rat ventricular myocyte (NRVM) culture and cell viability assay

The hearts of SD rats (one day old) were harvested, and blood stains were washed off using Hank's solution containing heparin. After mincing the hearts with scissors, the myocardial tissue was digested with 1% type II collagenase and trypsin without EDTA (2:1) for 5 min. The supernatant was collected, and the same digestion process was repeated until no tissue block was visible. The cells in the supernatant were placed into a culture flask and were settled for 1.5 h in the 37 ℃ incubator. The underlying adherent myocardium fibroblasts were discarded, and the upper cells were well dispersed and then cultured in a plate pre-moistened with 1% gelatin. Fresh medium was supplied the next day when a few cells started to beat; after 2–3 days, the neonatal rat primary cardiomyocytes matured and began to beat. For the experiments, control and HR groups were cultured in normal medium containing 1‰ DMSO. In the treatment group, cells were cultured in medium containing 8 μM CE and 0.1 μM nisoldipine for 12 h before inducing hypoxia for 5 h and reoxygenation for 12 h, and 8 nM Bay-K-8644 was added 2 h before HR.

Cell viability was measured using 3-[4,5 -dimethylthiazol-2-yl] − 2,5-diphenyl-tetrazolium bromide (MTT) assay. NRVMs were seeded into 96-well plates. After the different treatments, MTT (1 mg/mL) was added to the primary cells and incubated for 4 h at 37 ℃. The supernatant was discarded, and DMSO was added to dissolve the formazan crystals. The absorbance was measured at 570 nm using a Synergy H1 microplate reader (BioTek, Vermont, USA).

Detection of intracellular reactive oxygen species (ROS) in hiPSC-CMs

The experimental protocol of hiPSC-CM culture was the same as above. The level of intracellular ROS in hiPSC-CMs was detected using the ROS assay kit (Beyotime, Shanghai, China). Following different treatments, DCFH-DA (10 μM) probe was added to the cells for 30 min at 37 °C in the dark. Cells were washed three times to remove probes that did not enter [18]. Intracellular ROS level was reflected by the fluorescence intensity measured using the IncuCyte™ S3 ZOOM cell imaging system (Essen BioScience, Ann Arbor, MI).

Detection of intracellular calcium in hiPSC-CMs

The experimental protocol of hiPSC-CM culture was the same as above. Fluo-3 AM was used as fluorescent indicator to measure intracellular calcium levels. The cardiomyocytes were cultured to a confluence of ~ 80% and divided into groups. Then, cardiomyocytes were incubated in medium containing 5 μM Fluo-3AM at 37 °C in the dark for 40 min. After adding fresh medium, the cells were incubated for 20 min at 37 °C in the dark to generate calcium fluorescence [19]. Intracellular calcium levels were determined by the fluorescence images taken using IncuCyte™ S3 ZOOM cell imaging system (Essen BioScience, Ann Arbor, MI).

Immunofluorescence staining of rat cardiac tissue

The experimental protocols are shown in Fig. 4a. Rat hearts were embedded in paraffin and cut into 7–8 μm sections. Paraffin sections were placed at 60 °C for 1 h, dewaxed in xylene, and hydrated in alcohol gradient. The sections were then subjected to antigen retrieval by boiling in citrate buffer. Once restored at room temperature, the sections were blocked with BSA and incubated with primary antibody overnight at 4 °C. The next day, the sections were incubated with secondary antibody at 37 °C in the dark for 1 h, and nuclei were stained with DAPI [20,21]. The fluorescent images were acquired by Tissue Gnostics AX10 analysis system (Vienna, Austria). The primary antibodies in this article were used including: α1C (ab84814, 1:1000) and tubulin (ab6046, 1:2000) were purchased from abcam (Cambridge, UK); BAG3 (A14826, 1:500) and α2δ (A10315, 1:500) were purchased from ABclonal (Wuhan, China).

Immunohistochemistry for rat cardiac tissue

The experimental protocols are shown in Fig. 4a. Paraffin sections of rat hearts were used for immunohistochemistry using SP Rabbit & Mouse HPR kit (CoWin Biosciences, Beijing, China) according to the manufacturer's instructions [22]. Briefly, heart paraffin sections were incubated with normal goat serum after dewaxing, hydrating, and antigen retrieval. The sections were then incubated in a suitable primary antibody solution at 4 ℃ overnight, followed by incubation with the corresponding secondary antibody solution. Finally, the DAB working solution was used for colour development, and the nuclei were counterstained with haematoxylin. The images were acquired by Aperio S2 Leica Biosystem microscopy (Leica, Wetzlar, Germany). The primary antibodies in this article were used including: α1C (ab84814, 1:1000) were purchased from abcam (Cambridge, UK); BAG3 (A14826, 1:500) were purchased from ABclonal (Wuhan, China).

Western blot

Western blots were performed according to reported protocols [23,24]. Briefly, 50 μg of total proteins were loaded per lane, separated using 10% SDS-PAGE, and transferred to a nitrocellulose membrane. The membrane was blocked in 5% skim milk at room temperature for at least 2 h and then incubated in primary antibody overnight at 4 °C. After washing three times with TBST, membranes were incubated with the corresponding secondary antibody at room temperature for 2 h. Finally, the bands were visualised using an ECL kit (CW0049, CWBIO, Beijing, China). The primary antibodies in this article were used including: SERCA (ab2861, 1:1000), RyR2 (ab2868, 1:1000), NCX (ab177952, 1:1000), α1C (ab84814, 1:1000), calpain-2 (ab126600, 1:1000), STIM1 (ab57834, 1:1000), CaMKⅡ (ab22609, 1:1000), p-CaMKⅡ

(ab32678, 1:1000), p-PLB (ab15000, 1:1000), calmodulin (ab45689, 1:1000), Troponin I (ab52862, 1:1000) and tubulin (ab6046, 1:2000) were purchased from abcam (Cambridge, UK); FKBP12.6 (sc-376135, 1:200) and PLB (sc-393990, 1:200) were purchased from Santa Cruz Biotechnology (California, USA); BAG3 (A14826, 1:500), α2δ (A10315, 1:500), γ (A10014, 1:500) and β (A9304, 1:500) were purchased from ABclonal (Wuhan, China). The secondary antibodies in this article were used including: rabbit (ab6721, 1:2000) and mouse (ab6728, 1:2000).

Drug affinity responsive target stability (DARTS) assay

NRVMs were lysed in protein extraction buffer (CW2333, CWBIO, Beijing, China) with protease inhibitor (CW2200, CWBIO, Beijing, China), and proteins were quantified using a BCA kit (CW0014S, CWBIO, Beijing, China) according the instruction. Cell lysates were incubated with CE (200, 400, 800 μM) at room temperature for 1 h. The cell lysates then underwent proteolysis (25 μg/mL) at room temperature for 15 min. The enzymatic hydrolysis reaction was terminated by adding loading buffer and the lysates were detected by western blot analysis [25,26]. The primary antibodies in this article were used including: α1C (ab84814, 1:1000) were purchased from abcam (Cambridge, UK); BAG3 (A14826, 1:500) were purchased from ABclonal (Wuhan, China).

Co-Immunoprecipitation (co-IP)

Co-IP were performed according Pierce™ Co-Immunoprecipitation Kit (26149, Thermo Scientific™, MA, USA). Then, twenty micrograms of affinity-purified antibody were prepared for coupling by adjusting the volume to 200 μL. A Pierce spin column filled with AminoLink Plus coupling resin and diluted antibody was incubated on a rotator or mixer at room temperature for 2 h to ensure that the slurry remained suspended during incubation. The antibody was immobilised on resin after adding quenching buffer to the column. Then, tissue lysates and coupling resin were incubated with gentle mixing overnight at 4 °C. The target protein was eluted using elution buffer, and the eluant was then mixed with loading buffer and denatured. The results were analysed using western blot as described previously [27–29]. The primary antibodies in this article were used including: α1C (ab84814, 1:1000) were purchased from abcam (Cambridge, UK); BAG3 (A14826, 1:500) were purchased from ABclonal (Wuhan, China).

Statistical analysis

Data were collected and analysed blindly, and were presented as mean ± SEM. Statistical analyses were performed using GraphPad Prism 5.0. For the column diagrams, one-way ANOVA followed by Tukey's post-hoc test was used for multiple comparisons. For patch-clamp and Cardio ECR data, two-way ANOVA was used for multiple comparisons. The statistical significance was set at $P < 0.05$ (two-tailed).

Results

CE protects against MI/R injury in rats

To demonstrate the cardiac protective effects of CE in rats, we chose the MI/R injury model (Fig. 1a-b) [15]. Evans Blue/TTC staining showed that the myocardial infarct area/ area at risk of IR group was closer to 60%, which was reduced to 53%, 38%, and 43% by treatment with 7.5, 15, and 30 mg/kg CE, respectively (Fig. 1c-d).

M−mode echocardiography was used to determine the protective effects of CE on cardiac function and the results showed that 7.5, 15, and 30 mg/kg CE can significantly restore cardiac function (Fig. 1e). Analysis of troponin I and myocardial enzyme levels indicated that IR caused extensive myocardial damage, and that 15 mg/kg CE was the most effective dose against MI/R injury (Fig. 1f). HE staining revealed the pathological features of myocardial damage. The IR group manifested severe myocardial infarction, fibroblast proliferation, myocardial fibre necrosis, lymphocytic infiltration, and haemorrhage (Fig. 1g). In CE-treated groups, especially the 15 mg/kg group, myocardial infarction clearly improved, although it could not be reversed. Next, we chose CE 15 mg/kg to further analyse the expression of calcium regulators in cardiac tissue using western blotting. Compared with the sham group, the IR group showed lower expression of calcium transporters SERCA and NCX, leading to an increase in intracellular calcium levels. Instead, the expression of calcium transporters RyR2 and α1C increased, therefore augmenting intracellular calcium levels. However, treatment with CE (15 mg/kg) restored the expression of these calcium regulatory proteins to normal levels, including calcium transporters (SERCA, α1C, RyR2 and NCX) (Fig. 1 h). Together, these results indicate that CE could protect the heart against MI/R injury by regulating calcium cycling proteins.

CE recovers damaged ARVMs and intracellular calcium homoeostasis induced by MI/R injury

Following MI/R injury, rat hearts were separated by enzymatic hydrolysis, and the obtained cardiomyocytes with proper morphology and function were used to detect contraction and calcium transients [7,30]. In the CE + IR group, the resting sarcomere length (+dL/dt and -dL/dt) was significantly higher than in the IR group. By contrast, sarcomere shortening amplitude (TR90 and TPS) in the CE + IR group was significantly reduced, indicating the positive inotropic effects of CE (Fig. 2 a-b). Notably, in ARVMs, CE not only resumed cell contraction, but also improved calcium transients. In the IR group, resting calcium levels, time-to-50% peak $[Ca^{2+}]$, and intracellular calcium transient decay rate increased after MI/R injury, while calcium amplitude, -d $[Ca^{2+}]/dt_{max}$ and + d $[Ca^{2+}]/dt_{max}$ decreased (Fig. 2 c-d). However, after CE treatment, the indicators of calcium transients returned basically to the control group level.

CE protects against HR and MI/R injury by electrophysiology

To assess whether CE could regulate LTCC, we employed LTCC agonist Bay-K-8644 and the specific LTCC inhibitor nisoldipine. Bay-K-8644 significantly affected impedance and field potential indicators of hiPSC-CMs [31,32]. However, CE counteracted the changes induced by Bay-K-8644, mainly by increasing contraction amplitude, contraction and relaxation time, and field potential amplitude, as well as reducing beat rate and field potential duration (Fig. 3a). Moreover, CE promoted a much better recovery of the abnormal contraction and electrical signals in hiPSC-CMs than nisoldipine after Bay-K-8644 treatment. Subsequently, we examined the effects of CE, LTCC inhibitor, and LTCC agonist on the calcium channels using patch-clamp. Remarkably, CE inhibited the increase of $I_{Ca,L}$ induced by Bay-K-8644, showing a stronger inhibitory effect than nisoldipine (Fig. 3b), which directly proved that CE could inhibit LTCC activity.

The Cardio ECR system recorded the growth and development of hiPSC-CMs in real time, and the protective effect of CE was also reflected by the impedance and field potential recording of hiPSC-CMs. After 5 h of hypoxia, hiPSC-CMs were analysed by the Cardio

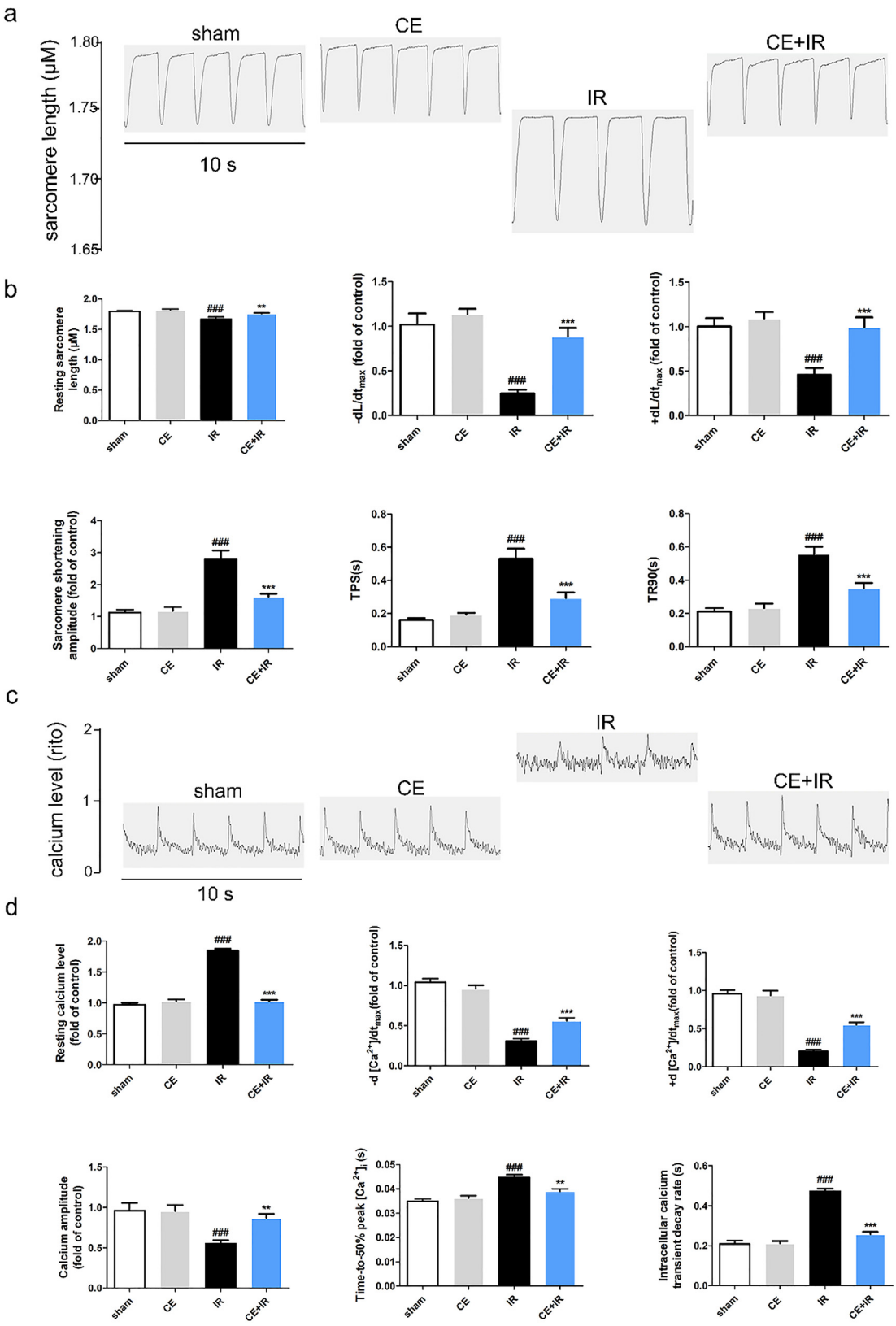

Fig. 2. CE regulated sarcomere contraction and calcium transient of ARVMs after MI/R injury. (a) The diagram (10 s) of sarcomere contraction. (b) The analysis results for CE's effect on sarcomere contraction of ARVMs and the indicators including resting sarcomere length, maximal velocity of re-lengthening (-dL/dt), maximal velocity of shortening (+dL/dt), sarcomere shortening amplitude, the time-to-peak shorting (TPS) and the time-to-90% re-lengthening (TR90) (n = 16 per group). (c) The diagram (10 s) of calcium transient (d) The analysis results for CE's effect on calcium transient of ARVMs and the indicators including resting calcium levels, calcium relaxation maximal velocity (-d [Ca^{2+}]/dtmax), calcium shorting maximal velocity (+d [Ca^{2+}]/dtmax), calcium amplitude, Time-to-50% peak [Ca^{2+}], intracellular calcium transient decay rate (n = 16 per group). The data were expressed as the mean ± SD. $^{###}$P < 0. 001 vs sham group; **P < 0.01 vs IR group, ***P < 0.001 vs IR group.

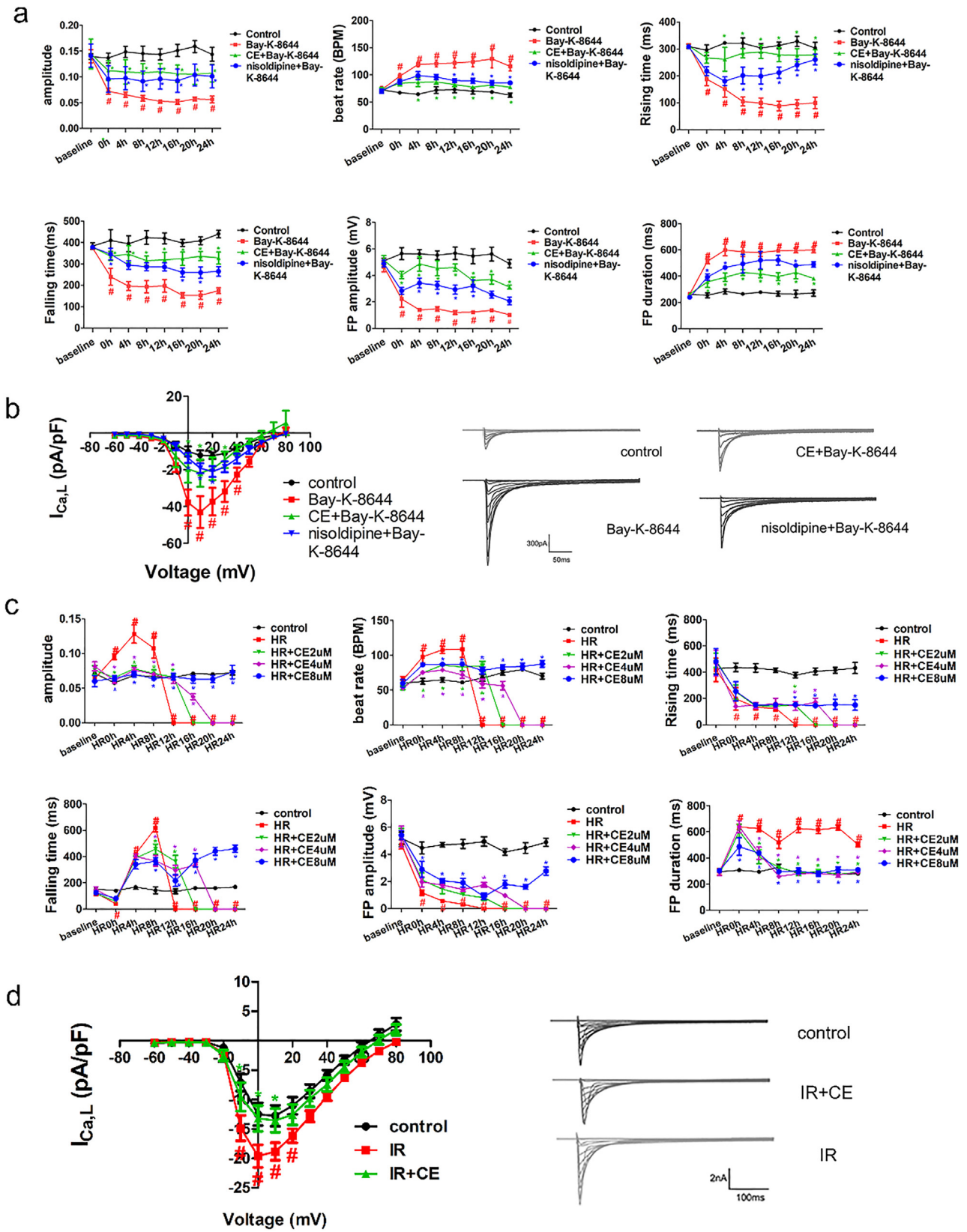

Fig. 3. Regulation of CE on LTCC by Cardio ECR and patch-clamp. (a) The impedance and field potential of hiPSC-CMs were real-time monitored after Bay-K-8644 treatment (n = 5 per group). (b) I–V curve (left) of Ca current and representative Ca current traces (right) recorded from the control group, Bay-K-8644 group, CE + Bay-K-8644 group, and nisoldipine + Bay-K-8644 group in hiPSC-CMs (n = 5 per group). The data were expressed as the mean ± SD. $^{\#}P < 0.05$ vs control group (The color of # was the same as the color of the curve); $^{*}P < 0.05$ vs Bay-K-8644 group (The color of * was same as the color of the curve). (c) After incubating CE for 24 h, hiPSC-CMs were hypoxic, and the impedance and field potential were monitored during reoxygenation 24 h (n = 5 per group). (d) After rat MI/R injury, NRVMs were obtained. Moreover, I–V curve (left) of Ca current and representative Ca current traces (right) recorded from the sham group, IR group, and CE + IR group. The data were expressed as the mean ± SD. $^{\#}P < 0.05$ vs control (sham) group (The color of # was same as the color of the curve); $^{*}P < 0.05$ vs HR (IR) group (The color of * was same as the color of the curve).

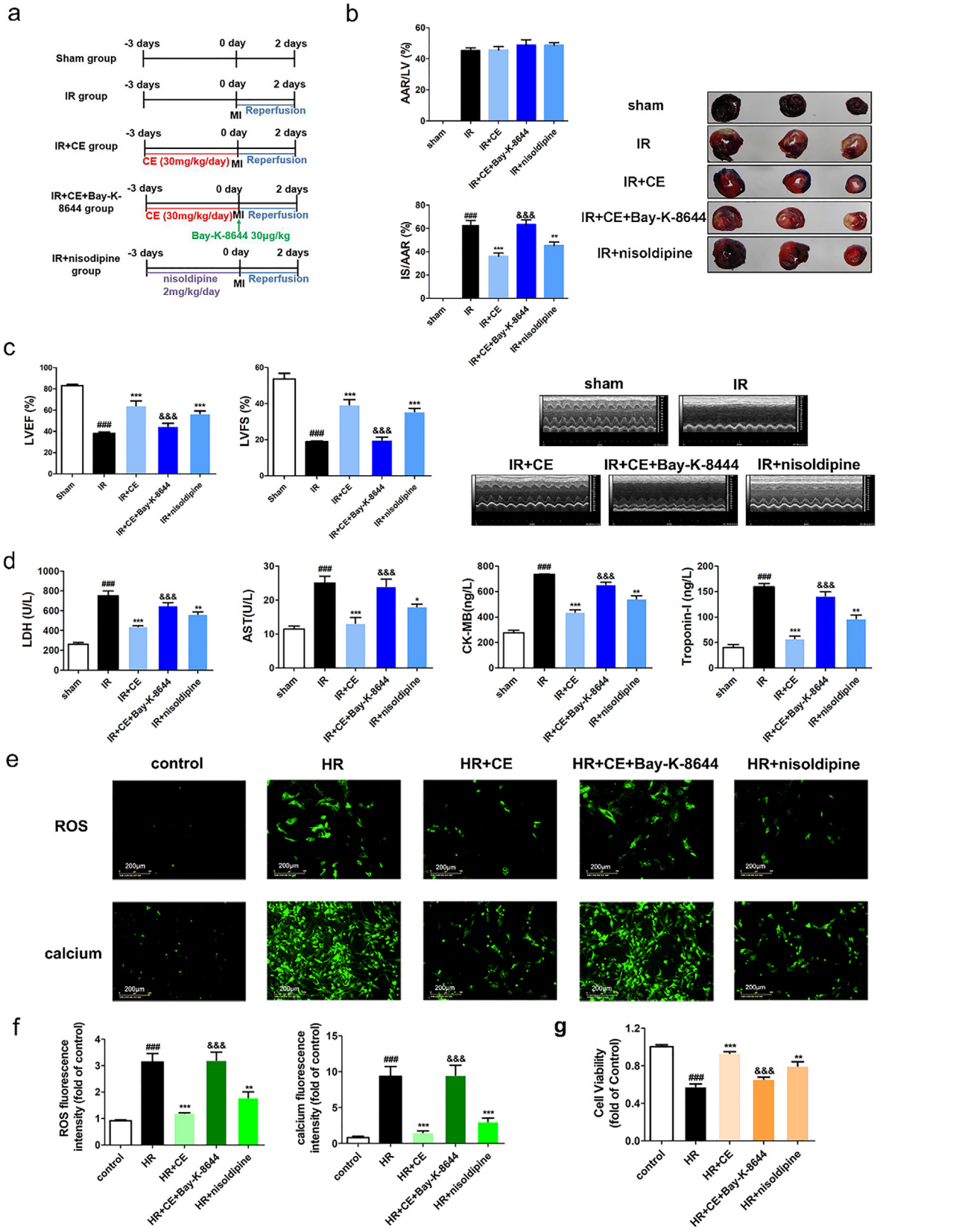

Fig. 4. CE alleviated MI/R injury by regulating LTCC in vivo and vitro. After treatment of CE (7.5, 15, 30 mg/kg) and nisoldipine (2 mg/kg) or Bay-K-8644 (30 μg·kg^{-1}) for three days, the rats were subjected to IR surgery. (a) Experimental protocol 2 to detect the effects of CE on MI/R injury in rat. (b) The myocardial infarction area was detected by Evans Blue/TTC staining, and quantification of infarct size (IS/AAR) and ischemic size (AAR/LV) was also displayed (n = 5 per group). (c) Representative trace of M−mode echocardiography performed 48 h after MI/R injury in a rat study and quantitative analysis of left ventricular ejection fraction (LVEF) and left ventricular fractional shortening (LVFS) using echocardiography (n = 5 per group). (d) The levels of LDH, AST, CK-MB, and Troponin-I were detected (n = 5 per group). (e) The fluorescence images of ROS and calcium levels (scale bar, 200 μm) in hiPSC-CMs were displayed after the treatment of nisoldipine (100 nM) or Bay-K-8644 (8 nM) (n = 6 per group). (f) The fluorescence intensity of ROS (left) and intracellular calcium (right) was statistically represented in the histogram. (g) After the intervention of nisoldipine (100 nM) or Bay-K-8644 (8 nM) for 2 h, NRVMs were incubated using CE (8 μM) for 12 h and then cell viability was detected after HR injury (n = 16 per group). The data were expressed as the mean ± SD. $^{###}$P < 0. 001 vs sham (control) group; *P < 0.05 vs IR (HR) group, **P < 0.01 vs IR (HR) group, ***P < 0.001 vs IR (HR) group; $^{\&\&\&}$P < 0.001 vs IR + CE (HR + CE) group.

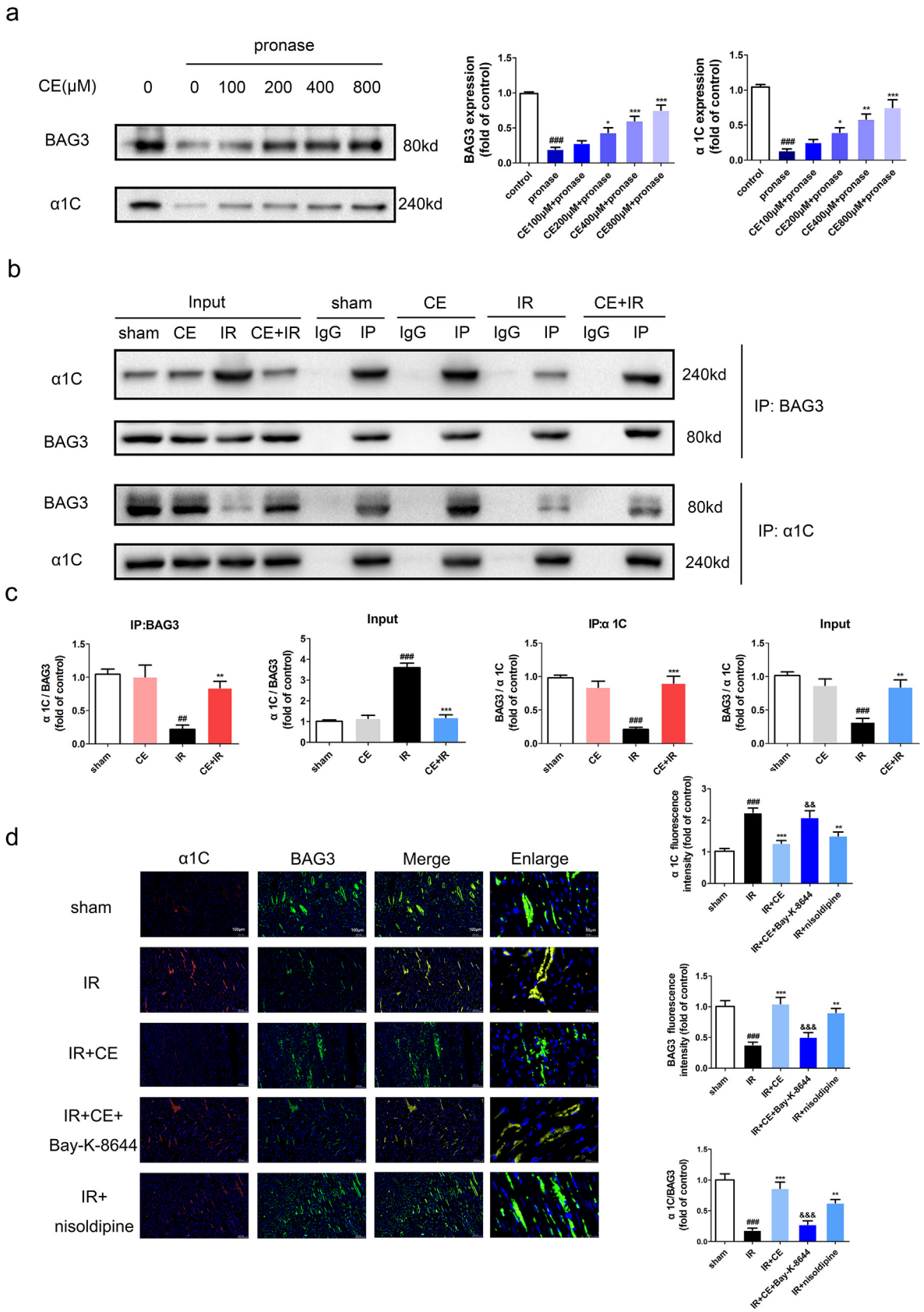

Fig. 5. CE promoted interaction between LTCC and BAG3. (a) DARTS assay is used to detect the effect of CE on BAG3 or α1C. Lysate of NRVMs was hydrolyzed by pronase after CE (0, 100, 200, 400, 800 μM) incubation 1 h. The expression of BAG3 and α1C were showed through western blots and statistical histograms (n = 5 per group). The data were expressed as the mean ± SD. $^{###}$P < 0. 001 vs control group; *P < 0.05 vs pronase group, **P < 0.01 vs pronase group, ***P < 0.001 vs pronase group. (b-c) Lysates (sham, CE, IR, CE + IR group) of rat heart tissue were co-immunoprecipitated using BAG3 or α1C antibody. The expression of BAG3 and α1C in input and IP were showed through western blots and statistical histograms (n = 5 per group). The data were expressed as the mean ± SD. $^{###}$P < 0. 001 vs sham group; **P < 0.01 vs IR group, ***P < 0.001 vs IR group. (d) Colocalization of BAG3 and α1C by immunofluorescence double staining were showed by the images (The scale bar is 100 μm or 20 μm.) and statistical histograms (n = 5 per group). The data were expressed as the mean ± SD. $^{###}$P < 0. 001 vs sham group; **P < 0.01 vs IR group, ***P < 0.001 vs IR group; $^{&&}$P < 0.01 vs IR + CE group, $^{&&&}$P < 0.001 vs IR + CE group.

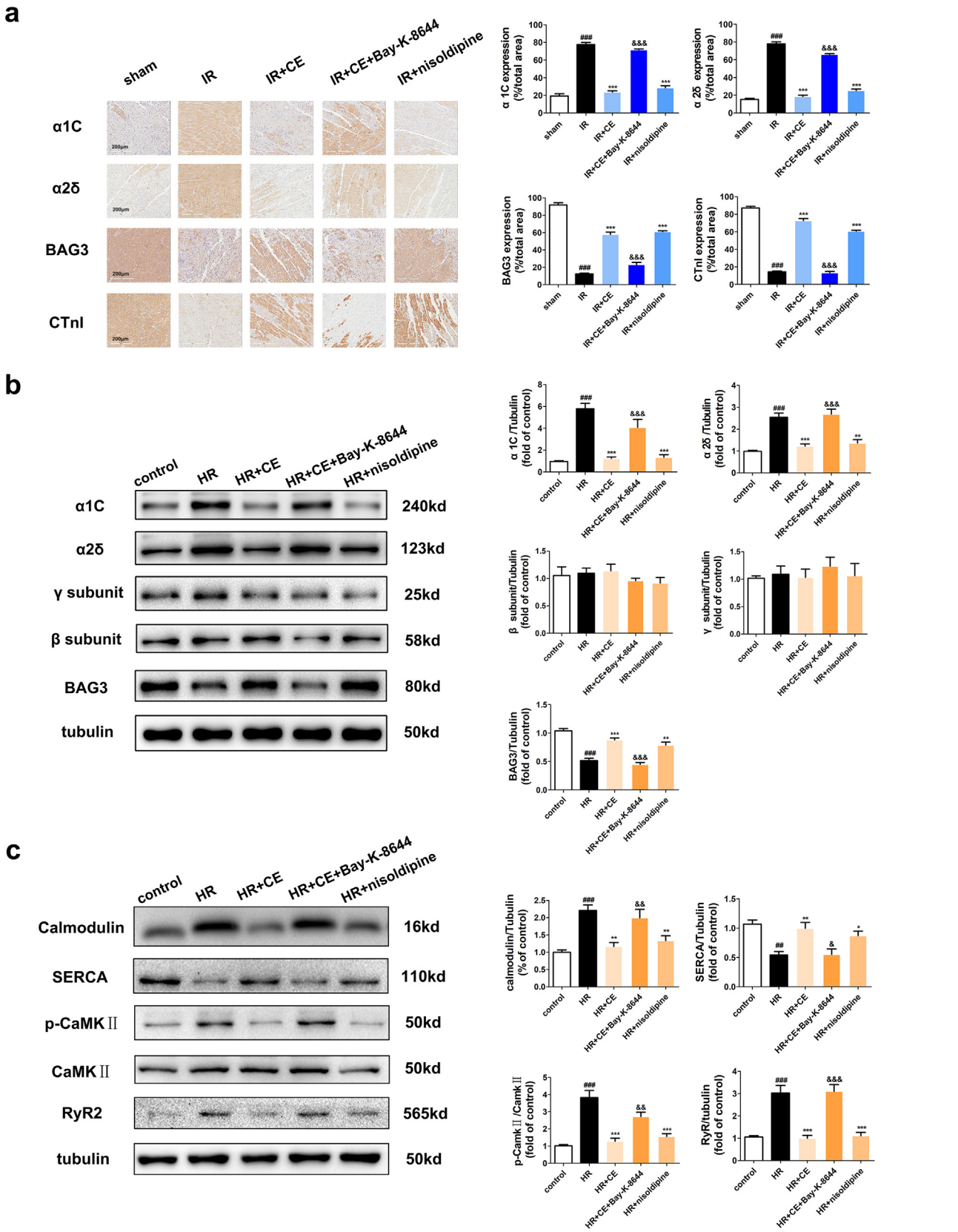

Fig. 6. Regulation of LTCC agonist on BAG3 and calcium pathway proteins. (a) The expression levels of α1C, α2δ, BAG3, and cardiac troponin I (CTnl) in rat myocardial tissue were displayed in immunohistochemical images and statistical histograms (n = 5 per group). (b) The expression levels of LTCC subunits (α1C, α2δ, γ, β) and BAG3 in NRVMs were displayed in western blots and statistical histograms (n = 5 per group). (c) The expression levels of Calmodulin, SERCA, CaMKⅡ and p-CaMKⅡ (T286) in NRVMs were displayed in immunohistochemical images and statistical histograms (n = 5 per group). The data were expressed as the mean ± SD. $^{\#\#}P < 0.01$ vs sham (control) group, $^{\#\#\#}P < 0.001$ vs sham (control) group; $^{*}P < 0.05$ vs IR (HR) group, $^{**}P < 0.01$ vs IR (HR) group, $^{***}P < 0.001$ vs IR (HR) group; $^{\&}P < 0.05$ vs IR + CE (HR + CE) group, $^{\&\&}P < 0.01$ vs IR + CE (HR + CE) group, $^{\&\&\&}P < 0.001$ vs IR + CE (HR + CE) group.

ECR system at the beginning of reoxygenation. As the reoxygenation time progressed, the beat rate, diastolic time, and field potential duration of hiPSC-CMs also increased, while the contraction time and field potential amplitude decreased rapidly. At 16 h of reoxygenation, the five indicators representing cellular function dropped to zero (Fig. 3c). These results indicated that, with prolonged reoxygenation time, damage in hiPSC-CMs continued to increase. Importantly, CE pre-treatment improved contraction and field potential function of hiPSC-CMs during HR; in particular, 8 μM CE restored cell functions to near-normal levels. Patch-clamp was used to further prove CE-mediated cardiac protection. For patch-clamp, ARVMs were isolated from rats who received MI/R 48 h after CE administration. In the IR group, $I_{Ca,L}$ increased considerably (Fig. 3d). Notably however, in the CE + IR group, $I_{Ca,L}$ was reduced to levels close to those of the sham group.

LTCC agonists influence CE's protective effect in vivo and vitro

To unveil the role of LTCC in MI/R injury, nisoldipine (2 mg/kg) and Bay-K-8644 (30 μg/kg) were administered to rats before myocardial ischemia surgery (Fig. 4a). As shown by Evans Blue/TTC staining, nisoldipine could reduce myocardial infarction size/area at risk (45.3%) compared to IR group, while Bay-K-8644 instead aggravated it (63.3%) (Fig. 4b). Echocardiographic results also showed that Bay-K-8644 obstructed cardiac protective effect of CE (Fig. 4c). Similarly, the levels of LDH, AST, CK-MB, and Troponin-I also demonstrated that activation of LTCC could exacerbate myocardial cell damage (Fig. 4d). Intracellular calcium levels are a direct measure of calcium overload. Therefore, we also detected intracellular calcium levels in hiPSC-CMs. Consistently, while Bay-K-8644 exacerbated intracellular calcium overload, both CE and nisoldipine instead reduced it (Fig. 4e-f). Analogously, analysis of intracellular ROS production indicated that Bay-K-8644 increased while CE and nisoldipine decreased oxidative stress, which is also closely connected to calcium overload. Importantly, these results were confirmed by analysis of NRVM viability after treatment. Bay-K-8644 treatment decreased the cell viability but nisoldipine increased it. (Fig. 4g).

CE enhances the interaction between LTCC and BAG3

Next, to clarify the molecular effects of CE and identify its potential targets, we employed DARTS. The principle of DARTS is that the binding of a compound to a target protein changes the conformation of the protein and improves its stability [25]. The levels of BAG3, which dropped sharply following protease hydrolysis, were gradually stabilised with higher concentrations of CE. Interestingly, the expression of α1C, the main functional subunit of LTCC, showed the same tendency as BAG3, suggesting that CE may interact directly with BAG3 and LTCC (Fig. 5a).

To verify the direct interaction between these components and their interplay with CE, we performed co-IP. As expected, both BAG3 and α1C could successfully co-precipitate each other. Interestingly, the expression of BAG3 or α1C was significantly lower in the IR group than in the sham group, indicating weaker interaction between these two proteins during ischemia. However, CE treatment could restore their interaction to normal levels (Fig. 5-b-c). Additionally, the interaction between BAG3 and LTCC was further confirmed by immunofluorescence. In line with the previous results, CE restored the interaction between BAG3 and α1C. Consistently, the LTCC inhibitor also restored this interaction, while the LTCC agonist reversed it. (Fig. 5d).

LTCC agonist reverses the effect of CE on the expression of LTCC and BAG3

Next, to elucidate the regulatory effect of CE on BAG3 and LTCC, we analysed their expression by western blot and immunohistochemistry. In the CE + IR group, the expression of LTCC subunits (α1C and α2δ, but not γ or β) increased after treatment with Bay-K-8644, whereas expression of BAG3 strongly decreased. Importantly, nisoldipine induced opposite effects to those of Bay-K-8644 (Fig. 6a-b). Immunohistochemistry showed consistent results for expression of LTCC subunits and BAG3. Finally, Bay-K-8644 also increased the expression of calmodulin, RyR2, and CaMKII (T286)/CaMKII but decreased that of SERCA (Fig. 6c). Collectively, these results demonstrate that CE could maintain calcium homeostasis by regulating LTCC and BAG3.

Discussion

In this study, we demonstrate that the natural compound CE plays a crucial role in cardiac protection. CE protected rats against MI/R injury by reducing myocardial infarct size and myocardial enzyme levels, as well as by ameliorating myocardial pathological damage and restoring cardiac function. In vitro, our team previously reported that CE analogues inhibit oxidative stress and apoptosis, thus protecting H9c2 cardiomyocytes [33]. Our current results also proved that CE improved cell viability of NRVMs after HR injury. Derived from human cells, hiPSC-CMs have similar mechanical and electrical activities to adult cardiomyocytes and are more reliable for evaluating cardiotoxicity than other cardiomyocytes, such as H9c2 [34]. We detected the impedance and field potential signals of hiPSC-CMs, which reflected visible contractile function and intrinsic ion channel signal, respectively [31]. Consistent with previous results, CE could mostly restore systolic and diastolic abnormalities and field potential signal weakness in a dose-dependent manner.

Complex mechanisms underlie MI/R injury. Currently, calcium overload is considered one of the crucial targets in this pathological process. Upon MI/R injury, excessive production of ROS causes cell membrane damage and increases membrane permeability, leading to extracellular Ca^{2+} influx and consequent increase in intracellular Ca^{2+} level [35]. Eventually, this results in intracellular calcium overload, which in turn causes contractile disorders and apoptosis [36,37]. Our data demonstrates that CE restores the systolic and diastolic function of ARVMs, which declined after MI/R injury. Importantly, CE also significantly reduced intracellular calcium overload caused by MI/R injury, especially during intracellular calcium transient decay. Calcium is a pivotal second messenger and plays a critical role in electrophysiology, excitation–contraction coupling, and contraction [38,39]. Therefore, the imbalance of intracellular calcium levels has a severe impact on numerous intracellular activities.

Several calcium cycling proteins are responsible for calcium transport and circulation in the cell, thereby ensuring intracellular calcium homeostasis [40,41]. Normally, opening of LTCC in cardiomyocytes causes extracellular Ca^{2+} influx, which triggers the release of Ca^{2+} by RyR2 on SR. Ultimately, this triggers contraction of cardiomyocytes mediated by increase in intracellular Ca^{2+} concentration. Subsequently, Ca^{2+} in the cytosol is retaken to the SR via SERCA and transported back to the extracellular space through NCX [42,43]. The decreased cytosolic Ca^{2+} concentration therefore induces myocardial cell relaxation. During MI/R injury, dysfunction of proteins that regulate intracellular calcium levels aggravates calcium overload in cardiomyocytes [3]. Our results show that CE upregulated SERCA and NCX and downregulated RyR2 and α1C, which substantially reduced calcium overload by recovering the

calcium in excess to the ER or/and transporting it outside the cell [44]. Therefore, we concluded that CE could protect against MI/R injury by reducing calcium overload.

In subsequent experiments, we found using RTCA Cardio ECR system that CE could recover the impedance and field potential signals of hiPSC-CMs after treatment with the LTCC agonist Bay-K-8644, suggesting that CE could inhibit calcium channels [31]. We verified this hypothesis using the patch-clamp technique, which allows to observe changes of cell membrane currents and to understand the activity of ion channels by analysing various factors, such as current intensity and channel opening/closing [45,46]. Patch-clamp analysis showed that CE significantly decreased the peak current of $I_{Ca,L}$ with Bay-K-8644 treatment. As expected, MI/R injury induced calcium overload, which was initiated by LTCC-mediated enhance in $I_{Ca,L}$ following ischemia [47]. Strikingly, calcium current increase was reversed by CE administration, demonstrating that CE reduced post-MI/R injury myocardial calcium overload by inhibiting LTCC activity. Calcium channels play an important role in maintaining the plateau of the action potential of cardiomyocytes. CE can reduce $I_{Ca,L}$, which also proves that CE can reduce the occurrence of arrhythmias by extending the duration of action potentials.

Nisoldipine is a dihydropyridine calcium channel blocker that is clinically used in the treatment of primary hypertension and coronary heart disease [11,12]. Bay-K-8644 is instead a highly selective LTCC agonist [48]. Here, unsurprisingly, administration of Bay-K-8644 aggravated the extent of myocardial injury notwithstanding CE treatment. Conversely, nisoldipine displayed a cardioprotective effect, but could ameliorate MI/R injury to a lower extent than CE. LTCC is a multi-subunit channel, containing the essential pore-forming subunit α1C, together with the auxiliary subunits and calmodulin [4,47]. The C-terminus of α1C is crucial for the channel trafficking of LTCC and is regarded as a target to modulate channel activity. Knockout of the β subunit in mice can slightly reduce the calcium current, while γ subunit exerts a typical effect on the amplitude of the calcium current. Notably, the $\alpha 2\delta$ subunit is essential to ensure the stability of the calcium current, and its knockout leads to a decrease in calcium current and prolonged inactivation time [38,47]. In our study, CE treatment before the MI/R injury increased the expression of α1C and $\alpha 2\delta$ but did not affect β and γ. Additionally, emerging evidence suggests that calmodulin can inhibit LTCC activity, while CaMKII can activate it, which also was proved by our results [49]. Enhanced LTCC activity leads to calcium overload, which can aggravate MI/R injury. In the SR, excessive RyR2 opening or weakened SERCA function can also exacerbate calcium overload [39]. Our data showed that LTCC could affect the amount of extracellular calcium entering the cell by modulating calcium channel activity, thereby influencing calcium transportation by other calcium cycling participants, and that CE can stabilise intracellular calcium homeostasis by regulating LTCC activity.

BAG3 is a 575-amino acid protein mainly expressed in the heart and skeletal muscle [50]. BAG3 enhances the anti-apoptotic effect of Bcl-2, thereby reducing cell damage under stress. Previous studies indicated that overexpression of BAG3 alleviates the degree of myocardial infarction due to MI/R [51]. Consistently, our results proved that CE could promote the expression of BAG3, reduce myocardial infarction in rats, and improve the viability of myocardial cells. Using the DARTS method, we demonstrated that CE treatment increased expression of LTCC and BAG3 dose-dependently, proving that this compound can directly act on these proteins. Importantly, our immunofluorescence results are consistent with those of previous reports showing that BAG3 and LTCC colocalise in the sarcolemma and transverse tubules, which implicates that BAG3-LTCC interaction plays a vital role in the intracellular calcium cycling of cardiomyocytes [50,52]. The direct interaction of LTCC with BAG3 was further confirmed through co-IP. This interaction, which was reduced due to MI/R injury, was fully restored after CE treatment, showing that CE could improve calcium homeostasis by promoting BAG3 and LTCC interaction. Co-localization data, however, showed that LTCC agonists can reduce the interaction between BAG3 and LTCC restored by CE. Collectively, our data demonstrate that CE protects against MI/R injury through significantly reducing intracellular calcium overload, which is achieved by enhancing BAG3-LTCC interaction.

This study proved that CE pre-administration can protect MI/R injury by regulating the interaction of LTCC-BAG3. However, there may be some possible limitations in this study. The effect of CE's therapeutic administration of on MI/R injury and its mechanism should be further explored in subsequent experiments. In fact, we have also carried out experiments to prove that both pre-administration and therapeutic administration of CE can significantly alleviate MI/R injury, and even the protective effect of CE pre-administration is better than CE's therapeutic administration (Supplementary Fig. 1), which is also main reason for the choice of CE pre-administration in the study. Of course, CE's therapeutic administration is also meaningful, and we will promote follow-up experiments.

Conclusion

In conclusion, we demonstrated that CE protects rats against MI/R injury and cardiomyocytes from HR injury by inhibiting calcium overload. Our findings showed that CE suppressed calcium overload by promoting the interaction between LTCC and BAG3, which stabilised calcium cycling in myocardial cells and thus promoted cardiac protection. These findings also provided a preclinical experimental basis for CE as a candidate drug for the treatment of MI/R injury.

Compliance with Ethics requirements

All Institutional and National Guidelines for the care and use of animals (fisheries) were followed.

Declaration of Competing Interest

The authors declare that they have no known competing financial interests or personal relationships that could have appeared to influence the work reported in this paper.

Acknowledgements

This work was supported by CAMS Innovation Fund for Medical Sciences (CIFMS) (No. 2016-I2M-1-012), the Drug Innovation Major Project (No. 2018ZX09711001-009), Central Public-Interest Scientific Institution Basal Research Fund (No. 2018PT35030) and the National Natural Science Foundation of China (No. 81603333).

Appendix A. Supplementary data

Supplementary data to this article can be found online at https://doi.org/10.1016/j.jare.2020.10.005.

References

[1] Wang C, Liu N, Luan R, Li Y, Wang D, Zou W, et al. Apelin protects sarcoplasmic reticulum function and cardiac performance in ischaemia-reperfusion by attenuating oxidation of sarcoplasmic reticulum Ca^{2+}-ATPase and ryanodine receptor. Cardiovasc Res 2013;100(1):114–24.
[2] Murphy E, Steenbergen C. Mechanisms underlying acute protection from cardiac ischemia-reperfusion injury. Physiol Rev 2008;88(2):581–609.
[3] Zhu S, Xu T, Luo Y, Zhang Y, Xuan H, Ma Y, et al. Luteolin Enhances Sarcoplasmic Reticulum Ca^{2+}-ATPase Activity through p38 MAPK Signaling

thus Improving Rat Cardiac Function after Ischemia/Reperfusion. Cell physiol biochem 2017;41(3):999–1010.
[4] Striessnig J, Bolz HJ, Koschak A. Channelopathies in Cav1.1, Cav1.3, and Cav1.4 voltage-gated L-type Ca^{2+} channels. Pflug Arch Eur J phy 2010;460(2):361–74.
[5] Maier LS, Bers DM. Calcium, Calmodulin, and Calcium-Calmodulin Kinase II: Heartbeat to Heartbeat and Beyond. J Mol Cell Cardiol 2002;34:919–39.
[6] Oda T, Yang Y, Uchinoumi H, Thomas DD, Chen-Izu Y, Kato T, et al. Oxidation of ryanodine receptor (RyR) and calmodulin enhance Ca release and pathologically alter, RyR structure and calmodulin affinity. J Mol Cell Cardiol 2015;85:240–8.
[7] Wang M, Tian Y, Du YY, Sun GB, Xu XD, Jiang H, et al. Protective effects of Araloside C against myocardial ischaemia/reperfusion injury: potential involvement of heat shock protein 90. J cell mol med 2017;21(9):1870–80.
[8] Wang R, Yang M, Wang M, Liu X, Xu H, Xu X, et al. Total Saponins of Aralia Elata (Miq) Seem Alleviate Calcium Homeostasis Imbalance and Endoplasmic Reticulum Stress-Related Apoptosis Induced by Myocardial Ischemia/Reperfusion Injury. Cell physiol biochem 2018;50(1):28–40.
[9] Wang S, Tian Y, Zhang JY, Xu HB, Zhou P, Wang M, et al. Targets Fishing and Identification of Calenduloside E as Hsp90AB1: Design, Synthesis, and Evaluation of Clickable Activity-Based Probe. Front pharmacol 2018;9:532.
[10] Tian Y, Wang S, Shang H, Wang WQ, Wang BQ, Zhang X, et al. The clickable activity-based probe of anti-apoptotic calenduloside E. Pharm biol 2019;57(1):133–9.
[11] Chen C, Chen W, Nong Z, Ma Y, Qiu S, Wu G. Cardioprotective Effects of Combined Therapy with Hyperbaric Oxygen and Diltiazem Pretreatment on Myocardial Ischemia-Reperfusion Injury in Rats. Cell physiol biochem 2016;38(5):2015–29.
[12] Mitrega KA, Nozynski J, Porc M, Spalek AM, Krzeminski TF. Dihydropyridines' metabolites-induced early apoptosis after myocardial infarction in rats; new outlook on preclinical study with M-2 and M-3. Apoptosis 2016;21(2):195–208.
[13] McGrath JC, Lilley E. Implementing guidelines on reporting research using animals (ARRIVE etc.): new requirements for publication in BJP. Br J Pharmacol 2015;172:3189–93.
[14] Zhang Q, Xiang J, Wang X, Liu H, Hu B, Feng M, et al. Beta(2)-adrenoceptor agonist clenbuterol reduces infarct size and myocardial apoptosis after myocardial ischaemia/reperfusion in anaesthetized rats. Br J Pharmacol 2010;160(6):1561–72.
[15] Wei B, Lin Q, Ji YG, Zhao YC, Ding LN, Zhou WJ, et al. Luteolin ameliorates rat myocardial ischaemia-reperfusion injury through activation of peroxiredoxin II. Br J Pharmacol 2018;175(16):3315–32.
[16] Koci B, Luerman G, Duenbostell A, Kettenhofen R, Bohlen H, Coyle L, et al. An impedance-based approach using human iPSC-derived cardiomyocytes significantly improves in vitro prediction of in vivo cardiotox liabilities. Toxicol appl pharmacol 2017;329:121–7.
[17] Luo L, Ning F, Du Y, Song B, Yang D, Salvage SC, et al. Calcium-dependent Nedd4-2 upregulation mediates degradation of the cardiac sodium channel Nav1.5: implications for heart failure. Acta physiol 2017;221(1):44–58.
[18] Bertero E, Maack C. Calcium Signaling and Reactive Oxygen Species in Mitochondria. Circ res 2018;122(10):1460–78.
[19] Lesnefsky EJ, Chen Q, Tandler B, Hoppel CL. Mitochondrial Dysfunction and Myocardial Ischemia-Reperfusion: Implications for Novel Therapies. Annu rev pharmacol toxicol 2017;57:535–65.
[20] Liu J, Wu P, Wang H, Wang Y, Du Y, Cheng W, et al. Necroptosis Induced by Ad-HGF Activates Endogenous C-Kit^{+} Cardiac Stem Cells and Promotes Cardiomyocyte Proliferation and Angiogenesis in the Infarcted Aged Heart. Cell physiol biochem 2016;40(5):847–60.
[21] Oliveira MS, Carmona F, Vicente WVA, Manso PH, Mata KM, Celes MR, et al. Increased Atrial beta-Adrenergic Receptors and GRK-2 Gene Expression Can Play a Fundamental Role in Heart Failure After Repair of Congenital Heart Disease with Cardiopulmonary Bypass. Pediatr cardiol 2017;38(4):734–45.
[22] Guo X, Cao W, Yao J, Yuan Y, Hong Y, Wang X, et al. Cardioprotective effects of tilianin in rat myocardial ischemia-reperfusion injury. Mol med rep 2015;11(3):2227–33.
[23] Ma HJ, Li Q, Ma HJ, Guan Y, Shi M, Yang J, et al. Chronic intermittent hypobaric hypoxia ameliorates ischemia/reperfusion-induced calcium overload in heart via Na^{+}/Ca^{2+} exchanger in developing rats. Cell physiol biochem 2014;34(2):313–24.
[24] Budas GR, Churchill EN, Disatnik MH, Sun L, Mochly-Rosen D. Mitochondrial import of PKCepsilon is mediated by HSP90: a role in cardioprotection from ischaemia and reperfusion injury. Cardiovas res 2010;88(1):83–92.
[25] Lomenick B, Hao R, Jonai N, Chin RM, Aghajan M, Warburton S, et al. In: Proceedings of the National Academy of Sciences of the United States of America. p. 21984–9.
[26] Sloan DD, Lam CY, Irrinki A, Liu L, Tsai A, Pace CS, et al. Targeting HIV Reservoir in Infected CD4 T Cells by Dual-Affinity Re-targeting Molecules (DARTs) that Bind HIV Envelope and Recruit Cytotoxic T Cells. PLoS pathog 2015;11(11):e1005233.
[27] Chemin J, Taiakina V, Monteil A, Piazza M, Guan W, Stephens RF, et al. Calmodulin regulates Cav3 T-type channels at their gating brake. J biol chem 2017;292(49):20010–31.
[28] Li J, Ruffenach G, Kararigas G, Cunningham CM, Motayagheni N, Barakai N, et al. Intralipid protects the heart in late pregnancy against ischemia/reperfusion injury via Caveolin2/STAT3/GSK-3beta pathway. J Mol Cell Cardiol 2017;102:108–16.
[29] Sun F, Duan W, Zhang Y, Zhang L, Qile M, Liu Z, et al. Simvastatin alleviates cardiac fibrosis induced by infarction via up-regulation of TGF-beta receptor III expression. Br J Pharmacol 2015;172(15):3779–92.
[30] Wang M, Sun GB, Zhang JY, Luo Y, Yu YL, Xu XD, et al. Elatoside C protects the heart from ischaemia/reperfusion injury through the modulation of oxidative stress and intracellular Ca(2)(+) homeostasis. Int J Cardiol 2015;185:167–76.
[31] Abi-Gerges N, Pointon A, Oldman KL, Brown MR, Pilling MA, Sefton CE, et al. Assessment of extracellular field potential and Ca(2+) transient signals for early QT/pro-arrhythmia detection using human induced pluripotent stem cell-derived cardiomyocytes. J Pharmacol Toxicol 2017;83:1–15.
[32] Ando H, Yoshinaga T, Yamamoto W, Asakura K, Uda T, Taniguchi T, et al. A new paradigm for drug-induced torsadogenic risk assessment using human iPS cell-derived cardiomyocytes. J Pharmacol Toxicol 2017;84:111–27.
[33] Tian Y, Du YY, Shang H, Wang M, Sun ZH, Wang BQ, et al. Calenduloside E Analogues Protecting H9c2 Cardiomyocytes Against H2O2-Induced Apoptosis: Design. Synthesis and Biological Evaluation. Front pharmacol 2017;8:862.
[34] Guo L, Eldridge S, Furniss M, Mussio J, Davis M. Use of Human Induced Pluripotent Stem Cell-Derived Cardiomyocytes (hiPSC-CMs) to Monitor Compound Effects on Cardiac Myocyte Signaling Pathways. Current protocols in chemical biology 2015;7(3):141–85.
[35] Li D, Wang X, Huang Q, Li S, Zhou Y, Li Z. Cardioprotection of CAPE- o NO 2 against myocardial ischemia/reperfusion induced ROS generation via regulating the SIRT1/eNOS/NF-κB pathway in vivo and in vitro. Redox Biol 2018;15:62–73.
[36] Chapoy-Villanueva H, Silva-Platas C, Gutierrez-Rodriguez AK, Garcia N, Acuna-Morin E, Elizondo-Montemayor L, et al. Changes in the Stoichiometry of Uniplex Decrease Mitochondrial Calcium Overload and Contribute to Tolerance of Cardiac Ischemia/Reperfusion Injury in Hypothyroidism. Thyroid 2019;29(12):1755–64.
[37] Zhu P, Hu S, Jin Q, Li D, Tian F, Toan S, et al. Ripk3 promotes ER stress-induced necroptosis in cardiac IR injury: A mechanism involving calcium overload/XO/ROS/mPTP pathway. Redox Biol 2018;16:157–68.
[38] Verkhratsky A, Parpura V. Calcium signalling and calcium channels: evolution and general principles. Eur J Pharmacol 2014;739:1–3.
[39] Hidalgo C. Calcium Rules. Circulation 2017;135:1379–81.
[40] Bers DM. Cardiac excitation–contraction coupling. Nature 2002;415:198–205.
[41] Capiod T. Cell proliferation, calcium influx and calcium channels. Biochimie 2011;93(12):2075–9.
[42] Stammers AN, Susser SE, Hamm NC, Hlynsky MW, Kimber DE, Kehler DS, et al. The regulation of sarco(endo)plasmic reticulum calcium-ATPases (SERCA). Can J Physiol Pharmacol 2015;93(10):843–54.
[43] Lou Q, Janardhan A, Efimov IR. Remodeling of calcium handling in human heart failure. Adv Exp Med Bio 2012;740:1145–74.
[44] Frank K, Kranias EG. Phospholamban and cardiac contractility. Ann Med 2000;32(8):572–8.
[45] Imoto K, Hirakawa M, Okada M, Yamawaki H. Canstatin modulates L-type calcium channel activity in rat ventricular cardiomyocytes. Biochem Biophys Res Commun 2018;499(4):954–9.
[46] Cho JH, Zhang R, Kilfoil PJ, Gallet R, de Couto G, Bresee C, et al. Delayed Repolarization Underlies Ventricular Arrhythmias in Rats With Heart Failure and Preserved Ejection Fraction. Circulation 2017;136(21):2037–50.
[47] Shaw RM, Colecraft HM. L-type calcium channel targeting and local signalling in cardiac myocytes. Cardiovasc Res 2013;98(2):177–86.
[48] Fass DM, Levitan ES. Bay-K-8644 Reveals Two Components of L-Type Ca 2+ Channel Current in Clonal Rat Pituitary Cells. J Gen Physiol 1996;108:1–11.
[49] Zhang R, Khoo MS, Wu Y, Yang Y, Grueter CE, Ni G, et al. Calmodulin kinase II inhibition protects against structural heart disease. Nat Med 2005;11(4):409–17.
[50] Feldman AM, Gordon J, Wang J, Song J, Zhang XQ, Myers VD, et al. BAG3 regulates contractility and Ca(2+) homeostasis in adult mouse ventricular myocytes. J Mol Cell Cardiol 2016;92:10–20.
[51] Myers VD, McClung JM, Wang J, Tahrir FG, Gupta MK, Gordon J, et al. The Multifunctional Protein BAG3: A Novel Therapeutic Target in Cardiovascular Disease. JACC Basic to translational science 2018;3(1):122–31.
[52] Knezevic T, Myers VD, Gordon J, Tilley DG, Sharp 3rd TE, Wang J, et al. BAG3: a new player in the heart failure paradigm. Heart Fail Rev 2015;20(4):423–34.